Structure and Electron Detachment Energies of Al_3P^- and $Al_3P_3^-$

Edet F. Archibong and Alain St-Amant*

Department of Chemistry, University of Ottawa, 10 Marie Curie, Ottawa, Ontario, Canada K1N 6N5

Sor Koon Goh and Dennis Marynick*

Department of Chemistry and Biochemistry, The University of Texas at Arlington, Box 19065, Arlington, Texas 76019

Received: December 31, 2001; In Final Form: April 12, 2002

An attempt is made to assign several of the peaks observed in the anion photodetachment photoelectron spectra of Al_3P^- and $Al_3P_3^-$ reported by Gómez, Taylor and Neumark [*J. Phys. Chem. A* **2001**, *105*, 6886]. For the Al_3P/Al_3P^- system, equilibrium geometries and harmonic vibrational frequencies are computed for several low-lying electronic states of the neutral molecule and the anion at the B3LYP, MP2, and CCSD(T) levels of theory using the 6-311+G(*2df*) one-particle basis set. Al_3P^- has a $^2B_2$ (C_{2v}) ground state, whereas a near degeneracy is found between the $^1A_1$ (C_{3v}) and $^1A_1$ (C_{2v}) states of the Al_3P molecule. The assignment of the Al_3P^- electron detachment spectrum is based on transitions from the $^2B_2$ (C_{2v}) ground state of the anion to neutral states with the same C_{2v} geometry. On the other hand, the adiabatic electron affinity (AEA) of Al_3P is computed as the difference in the total energies of the $^2B_2$ (C_{2v}) ground state of the anion and the $^1A_1$ (C_{3v}) ground state of the neutral. Its value is 1.76 eV at the CCSD(T) level. A value of 2.051 ± 0.020 eV reported as the AEA of Al_3P in the photoelectron study is assigned to the energy difference between the zero point vibrational levels of the $^2B_2$ (C_{2v}) state of the anion and $^1A_1$ (C_{2v}) state of the neutral. In the case of the $Al_3P_3^-/Al_3P_3$ system, the smallest basis set used is 6-311+G(*d*) and the largest is 6-311+G(*3df*). The anion has a $^2A_1'$ (D_{3h}) ground state that is well separated from other states, whereas, the $^1A_1'$ (D_{3h}) and the $^1A'$ (C_s) states of the neutral have almost the same energy. Vertical electron detachment energies (VEDE) computed for transitions originating from the $^2A_1'$ ground state of the anion to neutral states with the D_{3h} geometry are in very good agreement with the experimental photoelectron data. Assuming a $^1A_1'$ (D_{3h}) ground state, the AEA of Al_3P_3 is computed to be 2.39 eV at the CCSD(T) level. For a $^1A'$ (C_s) ground state, a value of 2.46 eV is obtained at the same level of theory. The experimental AEA of Al_3P_3 obtained from the photoelectron study is 2.450 ± 0.020 eV.

1. Introduction

Ab initio electronic structure calculations by Raghavachari and co-workers have established that two isomers of neutral Al_3P_3, one with a planar (D_{3h}) geometry **1** and the other with a face-capped trigonal bipyramid (C_s) geometry **2**, compete for the gas-phase equilibrium geometry of the molecule.[1] Using the quadratic configuration interaction technique including corrections for triple excitations [QCISD(T)] and a 6-31G* basis set, **1** was found to lie below **2** by roughly 7 kcal/mol. The QCISD(T) calculations were carried out with HF and MP2 optimized geometries. However, the inclusion of larger basis set effects (determined from the difference of the MP2/[6*s*,5*p*,2*d*,1*f*] and MP2/6-31G* results), reversed the stability predicted at the QCISD(T)/6-31G* level and **2** was found to be the ground-state geometry of Al_3P_3.[1] A subsequent study, which employed density functional theory within the local density approximation (DFT-LDA), also found **2** to be the most stable isomer of the aluminum phosphide trimer.[2] Using large flexible one-particle basis sets and the coupled cluster approach (CC), it is shown in the sections below that **1** and **2** of neutral Al_3P_3 are nearly isoenergetic as previously suggested and lie within 5 kcal/mol of each other. However, because we are interested in the electron detachment energies of $Al_3P_3^-$, the structure of the anion is cardinal because it dictates the structure of the neutral species accessed in a vertical Franck−Condon process such as anion photodetachment spectroscopy. To date, the literature is silent on the electronic structure calculations of $Al_3P_3^-$.

Using complete active space self-consistent field (CASSCF) and multireference singles and doubles configuration interaction (MRSDCI) methods, Feng and Balasubramanian have studied several low-lying electronic states of the Al_3P and AlP_3 molecules.[3] The authors reported a $^1A_1$ state with C_{3v} geometry as the ground electronic state of the Al_3P molecule. Due to Jahn−Teller distortion of the first ^3E excited state predicted at 1.86 eV by MRSDCI, the lowest excited state of the molecule was approximated to be at 1.6 eV above the ground state. According to the literature, geometric and electronic structure calculations of Al_3P^- have not been reported.

The Al_3P^-/Al_3P and $Al_3P_3^-/Al_3P_3$ systems are part of the $Al_xP_y^-$ ($x,y \leq 5$) clusters recently studied via anion photoelectron spectroscopy in Neumark's laboratory.[4] Included in the report are the vertical electron detachment energies (VEDE) corresponding to transitions from the lowest states of the anions to ground and low-lying electronic states of the neutral molecules, adiabatic electronic affinities (AEA), vibrational frequencies, and estimates of the electron affinities for cases where the 0−0 transition could not be determined precisely. In the photodetachment spectrum of Al_3P^-, three bands labeled X, A, and B are apparent at binding energies of 2.12, 2.99 and

10.1021/jp014669j CCC: $22.00
Published on Web 05/29/2002

Figure 1. Lowest energy isomers of Al_3P_3.

3.43 eV, respectively.[4] A vibrational progression with a frequency of 340 cm^{-1} is partially resolved for the X band, and the apparent position of the origin of the progression allows the AEA of Al_3P to be estimated as 2.051 ± 0.020 eV. Note that X is separated from states A and B by 0.87 and 1.31 eV, respectively. Unfortunately, these experimental results cannot be reconciled with earlier theoretical predictions[3] that place the lowest excited electronic states of Al_3P at 1.86 and 2.46 eV, respectively. We note that the latter is a careful and detailed MRSDCI study of the C_{3v} lowest energy isomer of Al_3P. Nonetheless, this discrepancy between the theoretical results[3] and experiment[4] clearly suggests that the C_{3v} form of Al_3P is not responsible for the main features in Al_3P^- photodetachment spectrum. In the case of the $Al_3P_3^-$ photoelectron spectrum,[4] two bands labeled X and A are evident at binding energies of 2.63 and 3.81 eV, respectively. The X band exhibits a resolved vibrational progression with a frequency of 630 cm^{-1} and the AEA is determined to be 2.450 ± 0.020 eV. In addition, the narrow width of the X band in the $Al_3P_3^-$ photodetachment spectrum indicates that the 2.63 eV transition involves two states with similar geometries. The question is which, if either, of the two lowest energy isomers of Al_3P_3 is observed in the anion photodetachment spectrum of $Al_3P_3^-$.

In light of the recent anion photodetachment experiments reported by Gómez, Taylor and Neumark,[4] it is appropriate to investigate the electronic structure of the Al_3P^- and $Al_3P_3^-$ clusters. A reexamination of the potential energy surface of Al_3P is necessitated by the significant difference (roughly 1 eV) in the theoretically predicted excitation energies,[3] and the experimental spectrum.[4] Low-lying isomers with energy very close to that of the ground-state structure have been known to account for several features observed in photodetachment spectra. In fact, we will establish in the sections below, via computations of the vibrational frequencies and the electron detachment energies (EDE), that a cyclic C_{2v} isomer (labeled **1** in Figure 2) is responsible for the recorded photodetachment spectrum of Al_3P^-. Our results also indicate that the **1**−C_{2v} form and the **3**−C_{3v} structure of Al_3P are very close in energy, and **1** is in fact the likely gas-phase equilibrium structure of Al_3P^-.

For the $Al_3P_3^-/Al_3P_3$ system, given the small energy separation between the D_{3h} ($^1A_1'$) and the C_s ($^1A'$) structures of the neutral molecule, an attempt is made to determine the isomer that is responsible for the observed photodetachment spectrum of $Al_3P_3^-$. Therefore, several stationary points on the potential surface of the anion are reported for the first time and the most stable isomers of the neutral are reexamined. Comparison of our results with those obtained from experiment allows for the identification of the main features observed in the $Al_3P_3^-$ spectrum.[4]

2. Computational Methods

The smallest one particle basis set used for the calculations on $Al_3P_3/Al_3P_3^-$ is 6-311G(*d*), and the largest is 6-311+G(*3df*). For the calculations on Al_3P/Al_3P^-, we use the 6-311+G(*2df*) basis. Note that for Al and P, the 6-311G(*d*) to 6-311+G(*3df*) basis sets are constructed from the McLean and Chandler (12s9p)/[6s5p] basis sets, augmented with polarization and diffuse functions.[5] Equilibrium geometries and vibrational frequencies are computed for all states using the hybrid B3LYP density functional[6,7] and the MP2 approximation[8] (for selected states). We then perform a series of CCSD(T)[9,10] single point energy calculations using the B3LYP and MP2 geometries, that is, CCSD(T)//B3LYP and CCSD(T)//MP2 calculations. In addition, geometries of the lowest lying states of Al_3P^-/Al_3P are also optimized at the CCSD(T) level. In the MP2 and CCSD(T) calculations, the 20 and 30 lowest molecular orbitals (MO) of Al_3P^-/Al_3P and $Al_3P_3^-/Al_3P_3$, respectively, are frozen. All computations have been performed with the GAUSSIAN 98 suite of programs.[11]

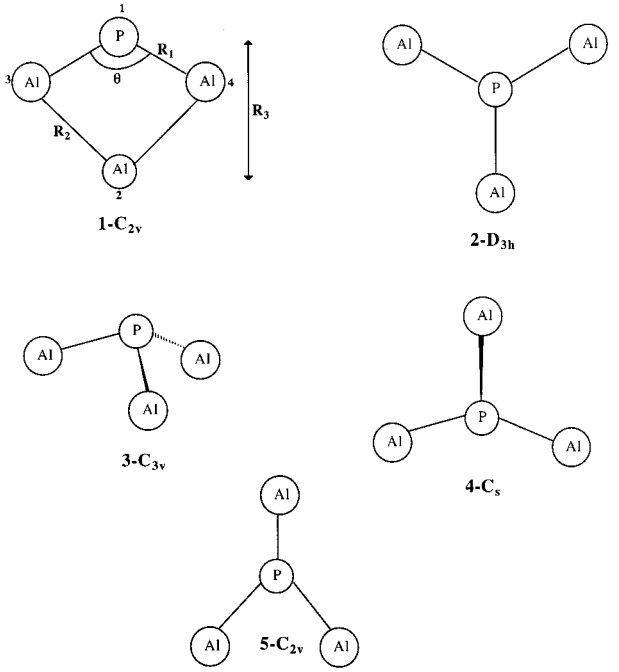

Figure 2. Geometry of Al_3P and Al_3P^- isomers reported in Table 2.

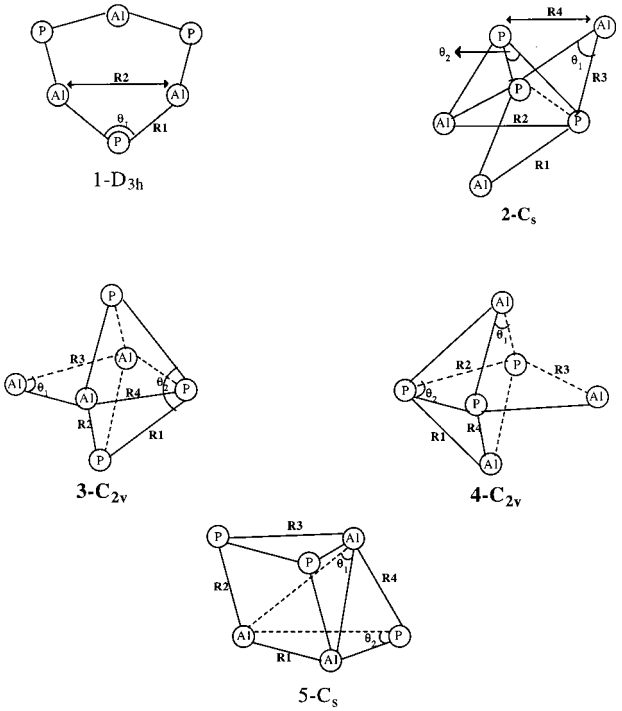

Figure 3. Geometry of Al_3P_3 and Al_3P_3- isomers reported in Table 4.

TABLE 1: Total Energies (a.u), Adiabatic Energy Separations (ΔE, eV), Adiabatic Electron Detachment Energies (AEDE, eV), Vertical Electron Detachment Energies (VEDE, eV) and the Adiabatic Electron Affinity (AEA, eV) for Al_3P^-/Al_3P

	method	structure	state	total energy	ΔE	AEDE	VEDE	AEA
Al_3P	CCSD(T)[a]	1-C_{2v}	$^3A_2$	−1066.824 329	1.71	3.53	3.76	
	CCSD(T)[b]			−1066.824 237	1.71	3.53	3.78	
	CCSD(T)						3.75	
	Expt.[c]						3.43	
	CCSD(T)[a]	1-C_{2v}	$^3A_1$	−1066.849 007	1.03	2.86	2.88	
	CCSD(T)[b]			−1066.848 435	1.03	2.88	2.87	
	CCSD(T)						2.88	
	Expt.[c]						2.99	
	CCSD(T)[a]	1-C_{2v}	$^3B_2$	−1066.855 369	0.86	2.69	2.88	
	CCSD(T)[b]			−1066.855 216	0.85	2.69	2.84	
	CCSD(T)						2.88	
	Expt.[c]						2.99	
	MP2	3-C_{3v}	$^1A_1$	−1066.827 358	0.17			1.73
	CCSD(T)[b]			−1066.889 491	−0.08			1.76
	CCSD(T)			−1066.889 497	−0.07			1.76
	B3LYP	2-D_{3h}	$^1A_1'$	−1068.743 099	−0.23			
	MP2			−1066.826 215	0.20			
	CCSD(T)[a]			−1066.888 474	−0.04			
	CCSD(T)[b]			−1066.888 510	−0.06			
	CCSD(T)			−1066.888 510	−0.04			
	B3LYP	1-C_{2v}	$^1A_1$	−1068.734 704	0.00	1.85	2.04	
	MP2			−1066.833 644	0.00	1.56	1.95	
	CCSD(T)[a]			−1066.887 007	0.00	1.83	2.04	
	CCSD(T)[b]			−1066.886 422	0.00	1.84	2.06	
	CCSD(T)			−1066.887 100	0.00	1.83	2.04	
	expt.[c]					2.05	2.12	
Al_3P^-								
	CCSD(T)[b]	1-C_{2v}	$^2A_2$	−1066.911 103	1.17			
	CCSD(T)[b]	1-C_{2v}	$^2B_1$	−1066.927 509	0.72			
	CCSD(T)[b]	5-C_{2v}	$^2A_1$	−1066.934 255	0.54			
	CCSD(T)[b]	4-C_s	$^2A'$	−1066.937 337	0.46			
	CCSD(T)[b]	1-C_{2v}	$^2A_1$	−1066.937 537	0.45			
	B3LYP	1-C_{2v}	$^2B_2$	−1068.802 593				
	MP2	1-C_{2v}	$^2B_2$	−1066.890 929				
	CCSD(T)[a]	1-C_{2v}	$^2B_2$	−1066.954 223				
	CCSD(T)[b]	1-C_{2v}	$^2B_2$	−1066.954 102	0.00			
	CCSD(T)	1-C_{2v}	$^2B_2$	−1066.954 236				

[a] Computed with B3LYP geometry. [b] Computed with MP2 geometry. [c] Ref 4.

3. Results and Discussion

The theoretical models used in this work have been tested in previous work on the electron detachment energies of GaP^-, GaP_2^-, AlP_2, $Al_2P_2^-$, and $Ga_2P_2^-$.[12−14] For these systems, the computed results are consistent with respect to the theoretical models and also in very good agreement with available experimental data. On the basis of previous performance, we believe these computational models are efficacious and should produce very reliable results in the current study. Unless specifically noted, the results listed in the Tables for the Al_3P^-/Al_3P systems are obtained with the 6-311+G(*2df*) one-particle basis set.

3.1. Al_3P and Al_3P^-. An extensive MRSDCI calculation has been performed on the C_{3v} isomer of Al_3P.[3] Because, the term energies computed in that work do not agree well with those obtained from the photoelectron spectrum of Al_3P^-,[4] we have examined other isomers of Al_3P as possible candidates for the species observed in the anion photodetachment experiment. The results of our calculations are presented in Tables 1 and 2, and the former includes experimental values for the VEDE. The B3LYP functional finds a $^1A_1'$ (**2**-D_{3h}) ground state for Al_3P with the $^1A_1$ (**1**−C_{2v}) state at 0.23 eV above, but it fails to locate the **3**−C_{3v} isomer. Optimization of the latter with the B3LYP functional always converged to **2**-D_{3h}. On the other hand, the MP2 approximation predicts that both $^1A_1$ (**3**−C_{3v}) and $^1A_1'$ (**2**-D_{3h}) states are 0.17 and 0.20 eV, respectively, higher in energy than the $^1A_1$(**1**−C_{2v}) state. Confronted with the inconsistency in the B3LYP and the MP2 results, and the small energy separation between the isomers, a more accurate relative energy is sought using the coupled cluster approach. First, CCSD(T) energies are computed using B3LYP and MP2 geometries. The results show that the CCSD(T)//B3LYP and the CCSD(T)//MP2 relative energies do not differ by more than 0.5 kcal/mol, in contrast to the10 kcal/mol difference found between B3LYP and MP2. Then, the geometries of **1**, **2**, and **3** are optimized at the CCSD(T) level. Inspection of Table 1 shows that the CCSD(T) calculations predict a near degeneracy between $^1A_1$ (**1**−C_{2v}), $^1A_1'$ (**2**-D_{3h}) and $^1A_1$ (**3**−C_{3v}) lowest-lying states of Al_3P. Vibrational frequency analyses indicate that $^1A_1$ (**1**−C_{2v}) and $^1A_1$ (**3**−C_{3v}) states are genuine minima whereas the $^1A_1'$ (**2**-D_{3h}) is a minimum on the B3LYP potential surface but a transition state for the inversion motion on the MP2 potential surface. The barrier for this inversion is about 0.7 kcal/mol at the CCSD(T) level. An important inference from the results listed in Table 1 is that $^1A_1$ (**1**−C_{2v}) and $^1A_1$ (**3**−C_{3v}) states are very close in energy, and there are few states of **1**−C_{2v} that are within 1.5 eV of the $^1A_1$ (**3**−C_{3v}) ground state. Those states with the C_{2v} geometry are responsible for the peaks observed in the photoelectron spectrum of Al_3P^- as discussed below.

With the CCSD(T) predictions that the $^1A_1$ (**1**−C_{2v}) state is within 2 kcal/mol of the $^1A_1$ (**3**−C_{3v}) ground state of Al_3P, we then sought the ground electronic state of Al_3P^-. Of course, strong candidates for the gas-phase equilibrium structure of the anion will include **1**−C_{2v} and **3**−C_{3v}. A $^2B_2$ (**1**−C_{2v}) [...$(4b_1)^2$-$(8b_2)^2(14a_1)^2(9b_2)^1$] state of Al_3P^- is formed if the $9b_2$ lowest unoccupied MO (LUMO) of $^1A_1$ (**1**−C_{2v}) is occupied by the attached electron. The vertical electron affinity (VEA) for the $^1A_1$ (**1**−C_{2v}) → $^2B_2$ (**1**−C_{2v}) process is 1.47 eV at the CCSD(T) level. In the case of **3**−C_{3v}, a ^2E state of the anion is expected

TABLE 2: Geometries (Å, degrees) and Vibrational Frequencies (cm^{-1}) and the Zero Point Energies (ZPE, kcal/mol) for the Low-Lying States of Al_3P^- and Al_3P

	Al_3P^-	Al_3P	Al_3P	Al_3P	Al_3P	Al_3P	Al_3P
B3LYP	$^2B_2$-(**1**-C_{2v})	$^1A_1$-(**1**)	$^3B_2$-(**1**)	$^3A_1$-(**1**)	$^3A_2$-(**1**)	$^1A_1'$-(**2**)	$^1A_1$-(**3**)
R_1	2.337	2.271	2.415	2.315	2.484	2.354	
R_2	2.721	2.637	2.794	2.822	2.793		
R_3	2.512	2.943	2.287	2.502	2.727		
θ	136.3	118.2	145.7	143.2	129.2		
ω_1	369 (a_1)	406	418	354	309	297 (a_1')	
ω_2	222 (a_1)	235	230	262	174	415 (e')	
ω_3	144 (a_1)	140	121	128	150	70 (e')	
ω_4	68 (b_1)	105	45	51	67*i*	20 (a_2'')	
ω_5	409 (b_2)	447	370	901	310		
ω_6	243 (b_2)	274	199*i*	317	226		
ZPE	1.69	2.30	1.69	2.88	1.67	1.84	
MP2							
R_1	2.338	2.290	2.422	2.278	2.473	2.345	2.353
R_2	2.750	2.560	2.809	2.852	2.804		
R_3	2.486	2.971	2.262	2.489	2.671		
θ	138.9	112.9	147.2	146.7	131.9		111.2
ω_1	381 (a_1)	413	477	388	328	310 (a_1')	339 (a_1)
ω_2	247 (a_1)	283	242	293	194	434 (e')	62 (a_1)
ω_3	127 (a_1)	170	114	143	129	54 (e')	415 (e)
ω_4	97 (b_1)	125	60	98	913	63*i*	68 (e)
ω_5	438 (b_2)	450	399	a	332		
ω_6	245 (b_2)	351	133	a	222		
ZPE	2.20	2.56	2.04		3.02	1.84	1.95
CCSD(T)							
R_1	2.343	2.283				2.345	2.354
R_2	2.716	2.620					
R_3	2.512	2.947					
θ	135.8	117.0					111.6

[a] Unphysical frequencies and intensities obtained for these modes.

to be formed but it will undergo Jahn−Teller distortion into the $^2A'$ and $^2A''$ states with C_s geometry. Both B3LYP and MP2 locate the $^2A'$-C_s state but optimization of the $^2A''$ geometry always finished with **1**−C_{2v}. The $^2A'$-C_s state of the anion is 0.46 eV above the ground state at the CCSD(T)//MP2 level. Several structures of doublet and quartet spin states have been optimized for the anion but none of them has a lower energy than **1**−C_{2v}. In short, our calculations find a $^2B_2$ (**1**−C_{2v}) ground electronic state for Al_3P^-.

3.1.1. Assignment of Al_3P^- Photoelectron Spectrum. Experimentally, the photoelectron spectrum of Al_3P^- shows three bands at 2.12 (X), 2.99 (A), and 3.43 (B) eV, corresponding to transitions to various electronic states of Al_3P. The estimate for the AEA is 2.051 ± 0.020 eV, and the data suggest that two excited states are 0.87 and 1.31 eV higher in energy than the ground electronic state. Our computed VEDE and the adiabatic electron detachment energies (AEDE) are included in Table 1.

The X band in the photodetachment spectrum is assigned to the $^1A_1$ (**1**−C_{2v}) + e^- ← $^2B_2$ (**1**−C_{2v}) [...$(4b_1)^2(8b_2)^2(14a_1)^2(9b_2)^1$] transition involving electron detachment from the $9b_2$ MO. Our calculated VEDE of 1.95, 2.04, and 2.04 eV at the MP2, B3LYP and CCSD(T) levels, respectively, agree very well with 2.12 eV obtained from experiment. The adiabatic electron detachment energy (AEDE) is computed to be 1.83 eV at the CCSD(T) level. A difference of 0.21 eV in the calculated VEDE and AEDE reflects the change in geometric parameters upon electron detachment to the $^1A_1$ (**1**−C_{2v}) states of the neutral molecule. The $9b_2$ MO from which an electron is removed consists essentially of the Al (p_y) orbitals and little contribution from P (p_y) (the molecule is on the $Y-Z$ plane with the Z-axis passing through Al and P). Using the B3LYP geometry in Table 2 (note the agreement with the CCSD(T) geometry), upon electron detachment, the Al−P (R_1) and Al−Al (R_2) bond distances are shortened roughly by 0.07 and 0.08 Å in the $^1A_1$ (**1**−C_{2v}) state compared to the $^2B_2$(**1**−C_{2v}) state. Consequently, the ω_1 (a_1) AlPAl symmetric stretching and the ω_2 (a_1) AlAlAl symmetric stretching/AlPAl bend have their frequency increased by 37 and 13 cm^{-1} in $^1A_1$ (**1**−C_{2v}). A frequency of 340 cm^{-1} associated with the X-band in the Al_3P^- photoelectron spectrum is assigned to the ω_1 (a_1) mode. The frequency of the latter at the B3LYP level is 406 cm^{-1}. The adiabatic electron affinity (AEA) of Al_3P is computed as the difference in the total energies of the $^2B_2$ (**1**−C_{2v}) ground state of the anion and the $^1A_1$ (C_{3v}) ground state of the neutral. A value of 1.76 eV is obtained at the CCSD(T) level for the AEA of Al_3P. Noteworthy, the AEA of 2.051 ± 0.020 eV reported in the photoelectron study[4] is obtained from the apparent origin of the 340 cm^{-1} progression associated with the X [$^1A_1$ (**1**−C_{2v})] band. On the basis of the assignment above, the 2.051 ± 0.020 eV value should correspond to the energy difference between the zero point vibrational levels of the $^2B_2$ (**1**−C_{2v}) and $^1A_1$ (**1**−C_{2v}) states. Note also that accurate AEA of Al_3P will be difficult to measure from the photoelectron experiment because the transition from the $^2B_2$ (**1**−C_{2v}) ground state of the anion to the $^1A_1$ (**3**−C_{3v}) ground state of the neutral involves a pronounced geometry change. This transition is unlikely to be observed in the photoelectron spectrum because of the small Franck−Condon factors associated with the large geometry difference between the anion and the neutral.

The A band observed at 2.99 eV can be assigned to overlap transitions to the $^3B_2$ (**1**−C_{2v}) and the $^3A_1$ (**1**−C_{2v}) states since identical VEDE of 2.88 eV is computed for the $^3B_2$ (**1**−C_{2v}) ← $^2B_2$ (**1**−C_{2v}) and the $^3A_1$ (**1**−C_{2v}) ← $^2B_2$ (**1**−C_{2v}) processes. A separation of 0.87 eV between the X and the A bands in the Al_3P^- electron detachment spectrum is consistent with 0.84 eV calculated at the CCSD(T) level. The $^3B_2$ state results from the removal of an electron from the $14a_1$ MO which largely consists of p_z atomic orbitals of P and Al(2). Electron detachment from the $8b_2$ MO [largely p_y orbitals of P, Al(3), Al(4) atoms] gives the $^3A_1$ state. Because these states and the $^2B_2$ anion ground state have the same molecular symmetry, the totally symmetric modes should be active upon photodetachment. This band is not vibrationally resolved in the recorded spectrum, but the computed frequencies of the three totally symmetric modes for each state are included in Table 2.

TABLE 3: Total Energies (a.u) and Relative Energies (eV) of the Lowest Energy Isomers of Al_3P_3 at Different Levels of Theory

	total energies		relative energies	
method	D_{3h}-($^1A_1'$)	C_s -($^1A'$)	D_{3h}	C_s
B3LYP/6-311G(d)	−1751.545 099	−1751.531 248	0.00	0.38
B3LYP/6-311+G(d)	−1751.548 735	−1751.536 570	0.00	0.33
B3LYP/6-311G(2d)	−1751.561 412	−1751.554 264	0.00	0.19
B3LYP/6-311+G(2d)	−1751.563 539	−1751.557 333	0.00	0.17
B3LYP/6-311+G(2df)	−1751.571 898	−1751.566 775	0.00	0.14
B3LYP/6-311+G(3df)	−1751.574 340	−1751.568 247	0.00	0.17
MP2/6-311G(d)	−1748.534 377	−1748.526 177	0.00	0.22
MP2/6-311+G(d)	−1748.542 248	−1748.539 040	0.00	0.09
MP2/6-311G(2d)	−1748.601 292	−1748.608 079	0.00	−0.18
MP2/6-311+G(2d)	−1748.606 013	−1748.614 153	0.00	−0.22
MP2/6-311+G(2df)	−1748.697 133	−1748.714 049	0.00	−0.46
MP2/6-311+G(3df)	−1748.703 673	−1748.714 178	0.00	−0.29
CCSD(T)/6-311G(d)[a]	−1748.603 063	−1748.592 086	0.00	0.30
CCSD(T)/6-311G(d)[b]	−1748.603 062	−1748.592 080	0.00	0.30
CCSD(T)/6-311+G(d)	−1748.611 586	−1748.605 081	0.00	0.18
CCSD(T)/6-311+G(d)[a]	−1748.611 593	−1748.605 087	0.00	0.18
CCSD(T)/6-311+G(d)[b]	−1748.611 592	−1748.605 097	0.00	0.18
CCSD(T)/6-311G(2d)[a]	−1748.671 930	−1748.672 320	0.00	−0.01
CCSD(T)/6-311G(2d)[b]	−1748.672 136	−1748.672 143	0.00	0.00
CCSD(T)/6-311+G(2d)[a]	−1748.677 071	−1748.678 812	0.00	−0.05
CCSD(T)/6-311+G(2d)[b]	−1748.677 295	−1748.678 608	0.00	−0.04
CCSD(T)/6-311+G(2df)[a]	−1748.777 371	−1748.781 731	0.00	−0.12
CCSD(T)/6-311+G(2df)[b]	−1748.777 375	−1748.781 543	0.00	−0.11
CCSD(T)/6-311+G(3df)[a]	−1748.784 502	−1748.781 991	0.00	0.07
CCSD(T)/6-311+G(3df)[b]	−1748.784 502	−1748.781 721	0.00	0.08

[a] Computed with B3LYP geometry. [b] Computed with MP2 geometry.

The B-Band observed at 3.43 eV in the Al_3P^- photodetachment spectrum is assigned to the $^3A_2$ (**1**−C_{2v}) state which results from detaching an electron from the $4b_1$ bonding MO. This MO is a delocalized π orbital comprising of the p_x (out of plane) orbitals of the four atoms. The VEDE calculated for the $^3A_2$ (**1**−C_{2v}) ← $^2B_2$ (**1**−C_{2v}) transition is 3.75 eV at the CCSD(T) level. It is worth noting that the $4b_1$ π bonding MO resembles the π orbital responsible for the stability of **1**−C_{2v} over **3**−C_{3v} in the valence 14-electron XAl_3^- (X = Si, Ge, Sn, and Pb) system and Al_4^{2-}.[15] Because the latter systems are planar, possess two delocalized π electrons and satisfy the $(4n+2)$ Huckel rule, suggestions have been made that they might be aromatic.[15−18] In this study, $^1A_1$ (**1**−C_{2v}) of Al_3P also has a planar geometry, possesses two delocalized π electrons and satisfies the $(4n+2)$ Huckel rule, and competes with $^1A_1$ (**3**−C_{3v}) for the ground electronic state of the neutral molecule. The question of the aromatic nature of M_3X (M = Al, Ga; X = P, As, Sb, Bi) will be addressed in a future publication.

3.2. Al_3P_3 and $Al_3P_3^-$. First, we consider the neutral molecule, Al_3P_3. Energies are listed in Table 3 whereas geometries and harmonic vibrational frequencies are included in Table 4. Despite the additional computational demands of our approach, which includes the study of basis set effects, the use of larger basis sets for geometry optimizations and the treatment of dynamic electron correlation at the CCSD(T) level,

TABLE 4: Geometries (Å, degrees) and Vibrational Frequencies (cm^{-1}) for the Low-Lying States of Al_3P_3 and $Al_3P_3^-$ at the B3LYP/6-311+G(*3df*) Level[a]

	$Al_3P_3^-$	Al_3P_3	Al_3P_3	$Al_3P_3^-$	$Al_3P_3^-$	$Al_3P_3^-$	$Al_3P_3^-$
B3LYP	$^2A_1'$ (1-D_{3h})	$^1A_1'$ (1-D_{3h})	$^1A'$ (2-C_s)	$^2A'$ (2-C_s)	$^2B_2$ (3-C_{2v})	$^2B_2$ (4-C_{2v})	$^2A'$ (5-C_s)
R_1	2.237	2.221	2.676	2.634	2.266	2.557	2.905
R_2	2.925	2.780	2.640	2.902	2.492	2.218	2.387
R_3			2.584	2.535	2.778	2.489	2.339
R_4			2.770	2.595	2.486	2.604	2.303
θ_1	81.6	77.5	51.4	51.8			61.4
θ_2	158.3	162.5	60.5	58.9			72.8
ω_1	365 (a_1')	381 (a_1')	516 (a')				
ω_2	254 (a_1')	324 (a_1')	418 (a')				
ω_3	510 (a_2')	507 (a_2')	349 (a')				
ω_4	572 (e')	603 (e')	296 (a')				
ω_5	289 (e')	327 (e')	264 (a')				
ω_6	142 (e')	202 (e')	219 (a')				
ω_7	160 (a_2'')	152 (a_2'')	156 (a')				
ω_8	123 (e'')	96 (e'')	82 (a')				
ω_9			385 (a'')				
ω_{10}			248 (a'')				
ω_{11}			141 (a'')				
ω_{12}			83 (a'')				

[a] Atomic coordinates of the isomers, at the various levels of theory reported in Tables 3 and 5, can be obtained from one of the authors at st-amant@theory.chem.uottawa.ca.

our conclusion based on the results presented in Table 3 is qualitatively similar to that reached by Raghavachari and coworkers. That is, the lowest $^1A_1'$-(D_{3h}) and the $^1A'$-(C_s) states of Al_3P_3 are nearly degenerate. Nonetheless, the following are noteworthy. With every basis set used (see Table 3), the B3LYP functional consistently predicts a $^1A_1'$-(D_{3h}) ground electronic state for Al_3P_3. On the other hand, the dependency of the MP2 and CCSD(T) energies on basis set size is very apparent. Enlargement of the basis sets appears to favor **2** at the MP2 level. Because DFT does not give a sufficient account of dynamic electron correlation and the exaggeration of the correlation effects within the MP2 approximation is recognized, a more complete treatment of electron correlation is undertaken at the CCSD(T) level using the B3LYP and MP2 geometries. Qualitatively, the trend in the relative energies at the MP2 and CCSD(T) levels are similar. However, with the more flexible basis sets [6-311+G(2d) to 6-311+G(3df)], CCSD(T) appears to favor **2** less than MP2 does, and eventually, both CCSD(T)//B3LYP and CCSD(T)//MP2 models place **1** below **2** by roughly 2 kcal/mol (~0.08 eV) when the 6-311+G(3df) basis is used. Although the preferred structure of the B3LYP functional is different from that of MP2, the relative energies computed with the CCSD(T)//B3LYP and CCSD(T)//MP2 models are consistent and do not differ by more than 0.3 kcal/mol for any of the basis sets. In other words, the B3LYP and the MP2 geometries are not significantly different for any given basis set. Faced with the frustration of not being able to establish the ground state of Al_3P_3 unequivocally from these extensive computations at the CCSD(T)//B3LYP and CCSD(T)/MP2 levels, a definitive conclusion is sought by optimizing **1** and **2** at the CCSD(T)/6-311+G(*d*) level. Though the latter computation is useful in the sense of geometry optimization at a level that incorporates sufficient dynamic electron correlation, it does not provide any additional insight, because the result is similar to that obtained at the CCSD(T)//B3LYP and CCSD(T)//MP2 levels using the same basis set. It is tempting to optimize the geometries of $^1A_1'$-(D_{3h}) and $^1A'$-(C_s) further at a higher level. However, the results in Table 3 clearly indicate that a meaningful result can only be achieved by using a very large flexible basis set. And even with a large scale optimization, there is no guaranty that the results will differ appreciably from that presented in Tables 3 and 4. We can only infer (and agree with earlier studies) that the lowest $^1A_1'$-(D_{3h}) and the $^1A'$-(C_s) states of Al_3P_3 are nearly degenerate and the results presented in the table suggest that the two states are likely to be within 0.2 eV (~5 kcal/mol) of each other. Furthermore, it is important to note that both the $^1A_1'$-(D_{3h}) and $^1A'$-(C_s) states are reasonably described by a single-reference correlation treatment. The T_1 diagnostic values obtained from the coupled cluster calculations are not greater than 0.025.

TABLE 5: Total Energy (a.u.) and the Relative Energies (ΔE, eV) of the Lowest States of $Al_3P_3^-$ at Different Levels of Theory

method	state	total energy	ΔE
B3LYP/6-311+G(2d)	5-$^2A''$	−1751.617 113	1.02
B3LYP/6-311+G(3df)	5-$^2A''$	−1751.625 439	1.05
MP2/6-311+G(3df)	5-$^2A''$	−1748.743 006	1.27
CCSD(T)[a]	5-$^2A''$	−1748.730 255	0.93
B3LYP/6-311+G(2d)	4-$^2B_2$	−1751.611 682	1.17
B3LYP/6-311+G(3df)	4-$^2B_2$	−1751.621 680	1.16
MP2/6-311+G(3df)	4-$^2B_2$	−1748.763 857	0.70
CCSD(T)[a]	4-$^2B_2$	−1748.732 980	0.85
B3LYP/6-311+G(2d)	3-$^2B_2$	−1751.619 346	0.96
B3LYP/6-311+G(3df)	3-$^2B_2$	−1751.628 776	0.96
MP2/6-311+G(3df)	3-$^2B_2$	−1748.772 550	0.47
CCSD(T)[a]	3-$^2B_2$	−1748.740 265	0.65
B3LYP/6-311+G(2d)	2-$^2A'$	−1751.600 805	1.46
B3LYP/6-311+G(3df)	2-$^2A'$	−1751.611 708	1.43
MP2/6-311+G(3df)	2-$^2A'$	−1748.749 666	1.09
CCSD(T)[a]	2-$^2A'$	−1748.718 079	1.26
B3LYP/6-311+G(2d)	1-$^2A_1'$	−1751.654 548	0.00
B3LYP/6-311+G(3df)	1-$^2A_1'$	−1751.664 157	0.00
MP2/6-311+G(3df)	1-$^2A_1'$	−1748.789 747	0.00
CCSD(T)[a]	1-$^2A_1'$	−1748.764 271	0.00

[a] Computed at B3LYP/6-311+G(2d) geometry.

Next we consider $Al_3P_3^-$. Ordinarily, an educated guess for the ground-state geometry of the $Al_3P_3^-$ anion will either be **1**-D_{3h} or **2**-C_s, because both are the lowest-lying quasi-degenerate isomers of the neutral molecule. Accommodation of one electron in the a_1' lowest unoccupied molecular orbital (LUMO) of the $^1A_1'$-(D_{3h}) state will result in a $^2A_1'$-(D_{3h}) state. For this process, a positive VEA of 2.24 eV is computed at the MP2/6-311+G(3df) level. In the case of the **2**-C_s ($^1A'$) isomer, the a' LUMO is expected to accommodate the added electron to give a $^2A'$ state. The VEA for this process is also positive with a value of 0.83 eV at the MP2/6-311+G(3df) level. Subsequent geometry optimizations of **1**-D_{3h} ($^2A_1'$) and **2**-C_s ($^2A'$) result in an energy separation of over 1.0 eV at all theoretical levels, and in favor of **1**. The energies of some of

TABLE 6: Electron Detachment Energies (eV) of Al_3P_3- and the Adiabatic Electron Affinity (AEA, eV) of Al_3P_3

	VEDE		AEDE	AEA
method	$1A_1' + e^- \leftarrow {}^2A_1'$	${}^3E'' + e^- \leftarrow {}^2A_1'$	$1A_1' + e^- \leftarrow {}^2A_1'$	$1A'$-C_s
B3LYP/6-311+G(3df)	2.55	3.55	2.44	2.61
MP2/6-311+G(3df)	2.47	4.07	2.34	2.06
CCSD(T)/6-311+G(2df)[a]	2.50	3.71	2.37	2.25
CCSD(T)/6-311+G(2df)[b]	2.50	3.71	2.37	2.25
CCSD(T)/6-311+G(3df)[a]	2.51	3.72	2.39	2.46
CCSD(T)/6-311+G(3df)[b]	2.48	3.73	2.39	2.46
Experiment[c]	2.63	3.81	2.450	

[a] Computed with B3LYP geometry. [b] Computed with MP2 geometry. [c] Ref 4.

the low-lying isomers of $Al_3P_3^-$ are listed Table 5. In this study, the gas-phase equilibrium geometry predicted for $Al_3P_3^-$ is **1**-D_{3h} ($^2A_1'$). Its geometrical parameters and harmonic vibrational frequencies, along with those of its neutral counterparts are included in Table 4.

3.2.1. Assignment of $Al_3P_3^-$ Photoelectron Spectrum. The electron photodetachment spectrum of $Al_3P_3^-$ shows two peaks at binding energies of 2.63(X) and 3.81(A) eV and an AEA of 2.450 ± 0.020 eV is reported for Al_3P_3. Assignment of the peaks is presented in Table 6. The X band is assigned to the $^1A_1'$-(D_{3h}) state of the neutral molecule. As discussed above, $Al_3P_3^-$ has a $^2A_1'$-(D_{3h}) ground electronic state and electron detachment from the highest occupied a_1' MO yields the $^1A_1'$-(D_{3h}) state. With the 6-311+G(*3df*) basis, the VEDE computed for the $^1A_1'$-(D_{3h}) $\leftarrow$ $^2A_1'$-(D_{3h}) transition are 2.55, 2.47, 2.51, and 2.48 eV at the B3LYP, MP2, CCSD(T)//B3LYP and CCSD(T)//MP2 levels, respectively. These computed VEDE are consistent with 2.63 eV obtained from the photoelectron experiment.[4] The results in Table 6 also show that the computed AEDE for this transition range from 2.34 eV (MP2) to 2.44 eV (B3LYP). The A band, on the other hand, is assigned to the $^3E''$ state which results from detaching an electron from the e'' HOMO-1 of the anion. The methods used in this work cannot adequately describe the $^3E''$ state because of its multireference character. Nonetheless, at the CCSD(T)/6-311+G(3df) level, the $^3E''$-(D_{3h}) $\leftarrow$ $^2A_1'$-(D_{3h}) transition has a computed VEDE of 3.73 eV, which may be suspect, that is in good agreement with the recorded peak at 3.81 eV. In the case of the AEA, our computed value is 2.39 eV, assuming a $^1A_1'$-(D_{3h}) ground state for Al_3P_3. Alternatively, in the footsteps of earlier calculations in which **2**-C_s ($^1A'$) appears to be the lowest energy isomer, then our computed AEA is 2.46 eV. Both the 2.39 eV [for $^1A_1'$-(D_{3h})] and the 2.46 eV [for $^1A'$-(C_s)] values bracket that obtained from experiment, that is, 2.450 ± 0.020 eV. It should be noted, however, that if Al_3P_3 indeed has a $^1A'$-(C_s) ground state, then the transition to this state from the $^2A_1'$-(D_{3h}) ground state of the anion would involve a huge geometry change, accompanied by very small Franck–Condon factors. Such transition would not be observed in the photoelectron spectrum, and in that case, the AEA of 2.450 ± 0.020 eV measured in the photoelectron study would not correspond to the true AEA of Al_3P_3. On the other hand, for a $^1A_1'$-(D_{3h}) ground state of Al_3P_3, the 2.450 ± 0.020 eV value [which appropriately is the AEDE of $^2A_1'$-(D_{3h})] would correspond to the true AEA.

4. Conclusions

The important features observed in the negative ion photoelectron spectra of Al_3P^- and $Al_3P_3^-$ have been assigned using quantum chemical methods. For Al_3P^-, the ground electronic state has a cyclic C_{2v} geometry. The ground-state geometry of neutral Al_3P is of the C_{3v} form but it has almost the same energy as the cyclic C_{2v} structure. The VEDE computed for Al_3P^- are in very good agreement with those obtained from its electron photodetachment spectrum.

A shortcoming of this study is that we are not able to pinpoint the ground state of Al_3P_3 despite extensive computational efforts. On the other hand, the goal of establishing **1**-D_{3h} as the species responsible for the $Al_3P_3^-$ photoelectron spectrum is achieved. The two peaks observed in the photodetachment spectrum of $Al_3P_3^-$ have been assigned to the $^1A_1'$-(D_{3h}) and the $^3E''$-(D_{3h}) states of Al_3P_3.

Acknowledgment. We wish to thank the Natural Sciences and Engineering Research Council of Canada and the University of Ottawa for financial support. Partial support of this work by grant Y-0743 from the Welch Foundation to DSM is gratefully acknowledged.

References and Notes

(1) Al-Laham, M. A.; Trucks, G. W.; Raghavachari, K. *J. Chem. Phys.* **1992**, *96*, 1137.
(2) Tomasulo, A.; Ramakrishna, M. *J. Chem. Phys.* **1996**, *105*, 10 449.
(3) Feng, P. Y.; Balasubramanian, K. *Chem. Phys. Lett.* **1999**, *301*, 458.
(4) Gómez, H.; Taylor, T. R.; Neumark, D. M. *J. Phys. Chem. A* **2001**, *105*, 6886.
(5) (a) McLean, A. D.; Chandler, G. S. *J. Chem. Phys.* **1980**, *72*, 5639. (b) Krishnan, R.; Binkley, J. S.; Seeger, R.; Pople, J. A. *J. Chem. Phys.* **1980**, *72*, 650. (c) Clark, T.; Chandrasekhar, J.; Spitznagel, G. W.; Schleyer, P. v. R. *J. Comput. Chem.* **1983**, *4*, 294. (d) Frisch, M. J.; Pople, J. A.; Binkley, J. S. *J. Chem. Phys.* **1984**, *80*, 3265.
(6) Becke, A. D. *J. Chem. Phys.* **1993**, *98*, 5648.
(7) Lee, C.; Yang, W.; Parr, R. G. *Phys. Rev. B* **1988**, *37*, 785.
(8) Hehre, W. J.; Radom, L.; Schleyer, P.v. R.; Pople, J. A. *Ab Initio Molecular Orbital Theor Theory*; Wiley: New York, 1986.
(9) Purvis, G. D.; Bartlett, R. J. *J. Phys. Chem.* **1982**, *76*, 1910.
(10) Raghavachari, K.; Trucks, G. W.; Pople, J. A.; Head-Gordon, M. *Chem. Phys. Lett.* **1989**, *157*, 479.
(11) Frisch, M. J.; Trucks, G. W.; Schlegel, H. B.; Scuseria, G. E.; Robb, M. A.; Cheeseman, J. R.; Zakrzewski, V. G.; Montgomery, J. A., Jr.; Stratmann, R. E.; Burant, J. C.; Dapprich, S.; Millam, J. M.; Daniels, A. D.; Kudin, K. N.; Strain, M. C.; Farkas, O.; Tomasi, J.; Barone, V.; Cossi, M.; Cammi, R.; Mennucci, B.; Pomelli, C.; Adamo, C.; Clifford, S.; Ochterski, J.; Petersson, G. A.; Ayala, P. Y.; Cui, Q.; Morokuma, K.; Malick, D. K.; Rabuck, A. D.; Raghavachari, K.; Foresman, J. B.; Cioslowski, J.; Ortiz, J. V.; Baboul, A. G.; Stefanov, B. B.; Liu, G.; Liashenko, A.; Piskorz, P.; Komaromi, I.; Gomperts, R.; Martin, R. L.; Fox, D. J.; Keith, T.; Al-Laham, M. A.; Peng, C. Y.; Nanayakkara, A.; Gonzalez, C.; Challacombe, M.; Gill, P. M. W.; Johnson, B. G.; Chen, W.; Wong, M. W.; Andres, J. L.; Head-Gordon, M.; E. S. Replogle, E. S.; Pople, J. A.; *Gaussian 98*, revision A9; Gaussian, Inc.: Pittsburgh, PA, 1998.
(12) Archibong, E. F.; St-Amant, A. *Chem. Phys. Lett.* **2000**, *316*, 151.
(13) Archibong, E. F.; Gregorius, R. M.; Alexander, S. A. *Chem. Phys. Lett.* **2000**, *321*, 253.
(14) Archibong, E. F.; St-Amant, A. *Chem. Phys. Lett.* **2000**, *330*, 199.
(15) Li, X.; Zang, H. F.; Wang, L. S.; Kuznetsov, A. E.; Cannon, N. A.; Boldyrev, A. I.; *Angew. Chem., Int. Ed.* **2001**, *40*, 1867.
(16) Jusélius, J.; Straka, M.; Sundholm, D. *J. Phys. Chem. A* **2001**, *105*, 9939.
(17) Fowler. P. W.; Havenith, R. W. A.; Steiner, E. *Chem. Phys. Lett.* **2001**, *342*, 85.
(18) Boldyrev, A. I.; Wang, L. S. *J. Phys. Chem. A* **2001**, *105*, 10759.